INTERNATIONAL SOCIETY FOR SOIL MECHANICS AND GEOTECHNICAL ENGINEERING

SIMSG | ISSMGE

Bored pile foundation response using seismic cone test data

Réponse des pieux à l'aide des données de piézocône sismique

Mayne P.W.
Georgia Institute of Technology, Atlanta GA USA

Woeller D.J.
ConeTec Investigations, Richmond, BC Canada

ABSTRACT: A closed-form elastic continuum solution is used to represent the upper and lower segment response of bored piles subjected to bi-directional Osterberg load testing. For geotechnical parameter input, seismic piezocone tests (SCPTu) are a most efficient and economical means because the penetrometer readings provide data for assessing the capacity of side and base components, while the shear wave velocity provides the fundamental stiffness for displacement analyses. A simple algorithm for modulus reduction is employed to allow nonlinear load-displacement-capacity behavior. A load test case study involving two levels of embedded O-cells for a large bridge in Charleston, South Carolina is presented to illustrate the approach.

RÉSUMÉ: Une solution analytique en élasticité est utilisée pour représenter la réponse des sections supérieures et inférieures de pieux forés soumis à des essais de chargement bidirectionnel Osterberg. Les essais sismiques utilisant des piézocônes (SCPTu) sont des moyens efficaces et économiques pour obtenir des paramètres géotechniques. Les mesures du pénétromètre sont généralement utilisées pour l'analyse du frottement latéral et de la capacité portante, tandis que les données de vitesse des ondes de cisaillement donnent le module de cisaillement initial lors de l'analyse des déplacements. Un algorithme simple pour la réduction du module est utilisé pour l'analyse non-linéaire du comportement charge - déplacement - capacité. Une étude de cas sur un essai de chargement Osterberg à deux niveaux effectué sur un grand pont situé à Charleston en Caroline du Nord est utilisée afin d'illustrer cette démarche.

KEYWORDS: bored piles, cone penetration, deep foundations, elastic solution, load tests, shear modulus, shear wave velocity

1 INTRODUCTION

The Osterberg load cell provides a novel alternative to conventional static load tests that either rely on large dead weight frames or anchored reaction beams. The O-cell occupies a minimal space in its setup, essentially the same space taken by the bored pile foundation itself (Osterberg 1998, 2000). In the original design, a single sacrificial hydraulic jack is situated at the pile base (O'Neill, et al. 1997). After concrete placement and curing, the jack is pressurized resulting in bi-directional loading to simultaneously mobilize end bearing downward while pushing the shaft segment upward (Fellenius, 2001). After loading, the O-cell is grouted to become part of the completed and working foundation. In fact, the O-cell can be positioned at mid-level elevations within the pile shaft to better match and optimize opposing segments. Moreover, multiple O-cells are now utilized to stage load separate pile segments and verify higher load capacities.

An elastic pile solution (Randolph and Wroth, 1978, 1979) is shown to accommodate the various O-cell configurations, as well as the more common top-down loading of bored piles. The results from seismic piezocone tests (SCPTu) are shown to be applicable for providing all the necessary input parameters to drive the computations and generate curves on the axial pile deformation response. A case study from South Carolina is used to illustrate the methodology.

2 ARTHUR RAVENEL BRIDGE

This newly-completed I-17 bridge over the Cooper River in Charleston, SC was supported by over 400 large bored pile foundations having diameters of 1.8 to 3 m and embedded lengths of between 45 to 72 m. The 4.0-km long cable-stayed concrete segmental bridge has a main span length of 471 m and connects the city of downtown Charleston with Drum Island and Mount Pleasant, replacing two old steel truss crossways known as the Pearman and Grace Memorial bridges.

In the region, all significant heavy building, port, and civil structures are founded on a deep overconsolidated formation termed the Cooper Marl that generally lies below elevations -15 to -20 m MSL (Camp, 2004). The uppermost soils consist of soft variable clays, loose sands, silts, and peats of Holocene age which are heterogeneous deposits from marine, deltaic, and alluvial origins

2.1 Cooper Marl

The Cooper marl is a marine deposit consisting of stiff green-gray sandy calcareous clay of Oligocene age that has been preconsolidated by erosional processes and natural cementation. The marl has a high calcite content on the order of 60 to 80 %.

Mean values of indices from laboratory tests include: w_n = 48%, w_L = 78%, and PI = 38% (Camp et al. 2002). Typical SPT-N values in the Cooper marl are between 12 and 16 blows/0.3 m. Triaxial tests consistently show high effective stress friction angles averaging $\phi' \approx 44° \pm 3°$. An equivalent prestress $\Delta\sigma_v' = (\sigma_p' - \sigma_{vo}') = 480$ kPa captures the general trend of preconsolidation stress (σ_p') which increases with depth, as well as corresponding profile of overconsolidation ratio (OCR = σ_p'/σ_{vo}') that decreases with depth (Mayne 2007a).

For the bridge project, approximately 45 rotary drilled borings and 55 SCPTu soundings were completed to depths of 55 m. Two representative SCPTu soundings are presented in Figure 1. The SCPTu is a particularly efficient and economical means for site exploration as it provides five separate readings on soil response with depth, including: cone tip resistance (q_t), sleeve friction (f_s), porewater pressures (u_2), time rate of dissipation (t_{50}), and downhole-type shear wave velocity (V_s).
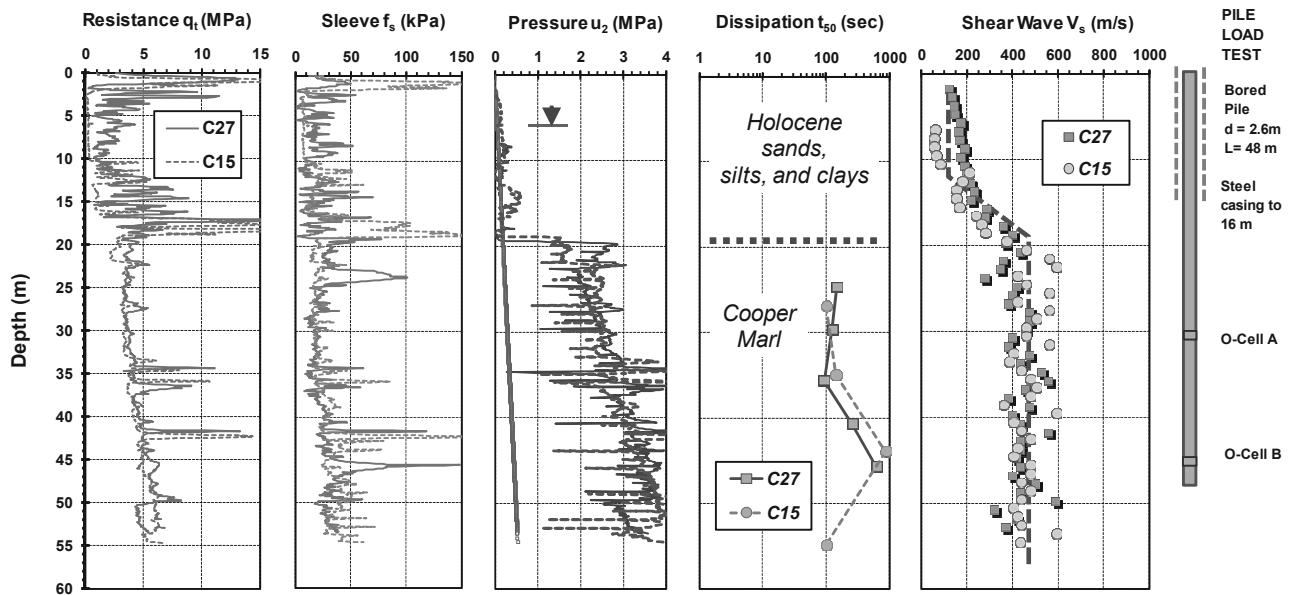
Figure 1. Soil profile with two representative seismic piezocone soundings (SCPTu) and O-cell setup for Arthur Ravenel Bridge, Charleston, SC

3 OSTERBERG LOAD TESTING

A fairly comprehensive load testing program of large diameter bored piles was performed at the site at the direction of the South Carolina Dept. of Transportation (Camp, 2004). This included 12 O-cell tests to measure static axial capacities and displacements. Three test sites were established to represent the conditions near Charleston, Drum Island, and Mount Pleasant.

The test setup for bored pile load test (MP-1) at the north end of the bridge at the Mt. Pleasant site had a constructed diameter d = 2.6 m and embedded length L = 48 m. The upper 16 m was cased with large diameter steel pipe to restrict load test results for pile side friction within the lower Cooper Marl. Two levels of Osterberg cells were installed at depths of 30 and 45 m to allow three-stages of loading.

The first stage involved pressurization of the lower O-cell resulting in a downward movement of the lower pile segment (d = 2.6 m; L = 2.53 m) while essentially no movement occurred in the upper shaft portions. Stage 1 involved base mobilization into the marl to evaluate end bearing resistance plus a small portion of side friction. The second stage involved pressurization of the upper O-cell with the lower cell ventilated (open). Stage 2 resulted in a downward motion of the mid-section shaft (d = 2.6 m; L = 14.0 m) with virtually no movements above the elevation -30 m mark. As such, stage 2 solely involved mobilization of the side friction in the Cooper Marl.

Finally, stage 3 was conducted by closing the lower O-cell and pressurizing the upper O-cell to push the top pile segment upward. Essentially no displacements were recorded in the lower pile portions (below -30 m). Stage 3 data provided information on the shear resistance in the Cooper marl in the non-cased zone from depth intervals from elev. -16 to -30 m.

4 EVALUATION OF AXIAL PILE RESPONSE

4.1 Pile Capacity Assessment

For pile capacity, CPT data can be utilized either directly or indirectly to assess the end bearing and side components (e.g., Eslami and Fellenius 1997; Mayne 2007b). Herein, a rational or indirect approach was followed using the CPT data to evaluate geotechnical parameters to determine the pile side friction (f_p) and base resistance (q_b).

For end bearing resistance of piles in clays, limit plasticity solutions detail that:

$$q_b \quad = \quad N_c \cdot s_u \tag{1}$$

where N_c = bearing factor (N_c = 9.33 for circular pile) and s_u = undrained shear strength. For a mode corresponding to direct simple shear (DSS), the strength can be obtained from:

$$s_u \quad = \quad \tfrac{1}{2} \sin\phi' \cdot OCR^\Lambda \cdot \sigma_{vo}' \tag{2}$$

where σ_{vo}' = effective overburden stress, exponent $\Lambda = 1 - C_s/C_c$ ≈ 0.8, C_s = swelling index, and C_c = compression index. In clays, an evaluation of the overconsolidation ratio from CPT data using the expression:

$$OCR \quad = \quad \tfrac{1}{3} Q \tag{3}$$

where $Q = (q_t-\sigma_{vo})/\sigma_{vo}'$ = normalized cone tip resistance. The CPT data indicate OCRs decreasing from 6 to 3 which are slightly higher than OCRs from the noted $\Delta\sigma_v'$ = 480 kPa.

The effective stress friction angle in clays can be evaluated from piezocone results using an effective stress limit plasticity solution developed by Senneset, et al. (1989). A simplified form can be expressed (Mayne, 2005):

$$\phi' \quad = 29.5° \cdot B_q{}^{0.121} \, [0.256 + 0.336 \cdot B_q + \log Q] \tag{4}$$

where $B_q = (u_2-u_0)/(q_t-\sigma_{v0})$ = normalized excess porewater pressure. The equation is applicable for the following ranges: $20° \le \phi' \le 45°$ and $0.1 \le B_q \le 1.0$. For the Cooper Marl, the CPTu results indicate an effective $\phi' \approx 43°$, quite comparable to values measured from laboratory CIUC triaxial tests on undisturbed samples (Mayne 2005).

The corresponding calculated values of pile end bearing resistance using equations (1) through (4) are presented in Figure 2 as a function of σ_{vo}'. The q_b increase from 2 to 4 MPa and compare quite well with the measured values evaluated from the O-cell test results.

The pile side resistance (f_p) can be expressed in terms of the lateral stress coefficient (K_0) and interface friction between the pile surface and surrounding soil. As a first approximation, this "beta" method gives:

$$f_p \approx K_0 \cdot \sigma_{vo}' \cdot \tan\phi' \qquad (5)$$

For soils with stress history of virgin loading-unloading, the geostatic lateral stress coefficient can be evaluated from:

$$K_0 = (1-\sin\phi') \cdot OCR^{\sin\phi'} \qquad (6)$$

In consideration of pile material type and method of installation, the expression is modified to:

$$f_p \approx C_M \cdot C_K \cdot K_0 \cdot \sigma_{vo}' \cdot \tan\phi' \qquad (7)$$

where C_M = interface roughness factor (= 1 for bored cast-in-place concrete, 0.9 prestressed concrete, 0.8 for timber, and 0.7 for rusty steel piles) and C_K = installation factor (= 1.1 for driven piles; 0.9 for bored piles).

Calculated values of pile side friction are shown in Figure 3 and vary between $150 < f_p < 250$ kPa. These are comparable in magnitude, and in some cases less than f_b determined from the O-cell load test series.
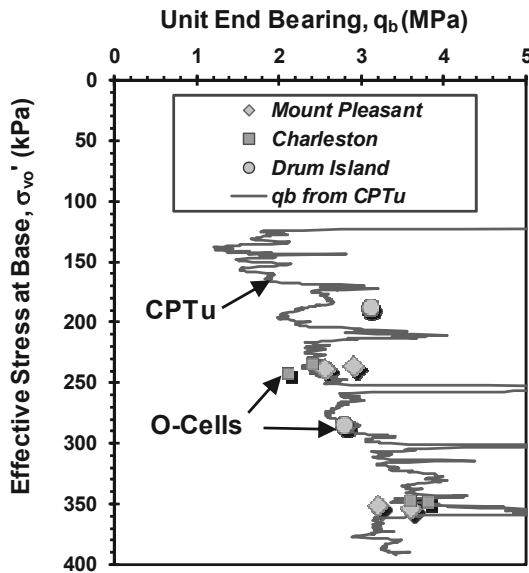

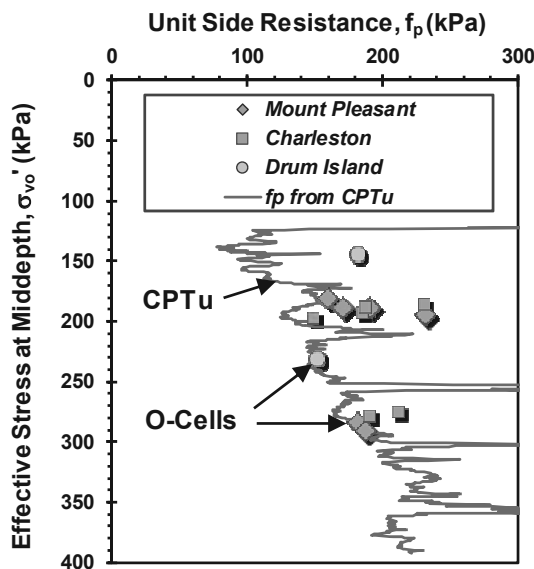Figure 2. Measured and calculated unit end bearing resistances

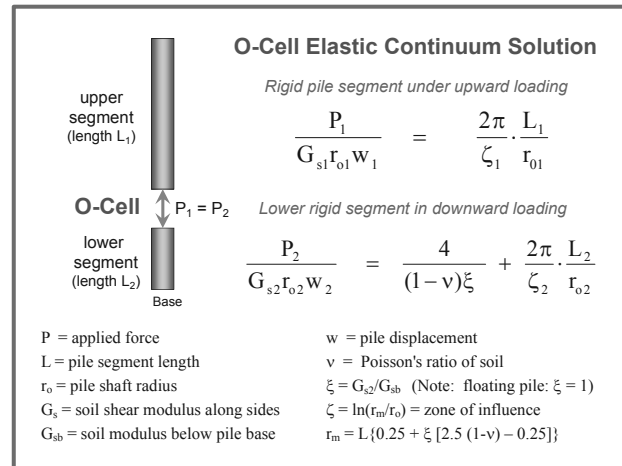Figure 3. Measured and calculated unit side friction resistances

Figure 4. Elastic continuum solution for O-cell loading of piles

4.2. *Axial Pile Displacements*

The elastic continuum solutions for an axial pile foundation are detailed by Randolph and Wroth (1978, 1979) and Fleming et al. (1992) by coupling a pile shaft with a circular plate. This can be deconvoluted back into the separate components to represent the original O-cell arrangement or into stacked pile segments for a mid-shaft O-cell as well as for multi-staged O-cell setups. For the simple case of rigid pile segments, Figure 4 presents the elastic solution for a mid-section O-cell framework.

The stiffness of the surrounding soil is represented by a shear modulus (G). The initial fundamental small-strain shear modulus of the ground is obtained from the shear wave velocity measurements:

$$G_0 = \rho_T \cdot V_s^2 \qquad (8)$$

where ρ_T = total mass density of the soil. This small-strain stiffness is within the true elastic region of soil corresponding to nondestructive loading. To approximately account for non-linearity of the stress-strain-strength behavior of soils, a modified hyperbola is adopted (Fahey, 1998):

$$G = G_0 \cdot [1 - (P/P_{ult})^g] \qquad (9)$$

where P = applied force, P_{ult} = axial capacity of the pile segment, and the exponent "g" is a fitting parameter (Mayne, 2007a, 2007b). Thus when P = 0, initially $G = G_0$ and at all higher load levels the shear modulus reduces accordingly.

Data from monotonic loading in resonant column, torsional shear, and triaxial shear tests with local strain measurements on both clays and sands under drained and undrained conditions have been compiled to evaluate the nonlinear modulus trends. A summary of these data for a wide variety of soils has been compiled and presented in Figure 5 (Mayne 2007b). The y-axis (G/G_0) can be considered as a modulus reduction factor to apply to the measured small-strain stiffness attained from (8) using site-specific V_s field data. The x-axis $(q/q_{max} = 1/FS)$ is a measure of the mobilized strength and can be considered as the reciprocal of the factor of safety (FS) corresponding to the load level relative to full capacity. In the case of pile capacity, the mobilized strength is obtained from the ratio of applied load to capacity $(P/P_{ult} = 1/FS)$

The modified hyperbola given by (9) is also presented in Figure 5 and can be seen to take on values of "g" exponent ranging from 0.2 (low) to 0.5 (high) when compared to the lab data. Usually, a representative exponent value g = 0.3 has been
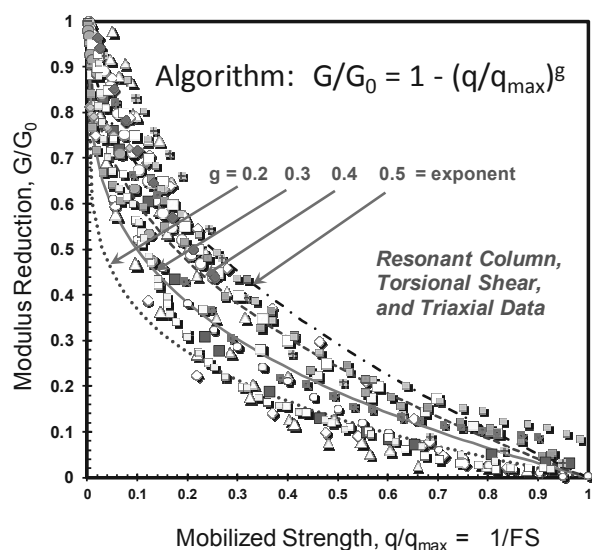
Figure 5. Modulus reduction algorithm for monotonic static loading

5 CONCLUSIONS

The upward and downward pile segments of an O-cell load test can be conveniently represented by a versatile elastic continuum solution. Results from seismic piezocone testing (SCPTu) provide the necessary input data to evaluate axial side and base resistances of the deep foundations, as well as the small-strain stiffness (G_{max}) needed for deformation analyses. Modulus reduction is dependent upon mobilized capacity ($P/P_{ult} = 1/FS$) using a simple algorithm. A case study involving a two-level O-cell arrangement for a large bored pile situated in the calcareous Cooper marl formation of South Carolina was presented to illustrate the application.

ACKNOWLEDGMENTS

REFERENCES

Camp, W.M. 2004. Drilled and driven foundation behavior in a calcareous clay. *GeoSupport 2004* (GSP 124), ASCE, Reston, Virginia: 1-18.

Camp, W.M., Mayne, P.W., and Brown, D.A. 2002. Drilled shaft axial design values in a calcareous clay. *Deep Foundations 2002*, Vol. 2, GSP No. 116, ASCE, Reston/Virginia: 1518-1532.

Eslami, A. and Fellenius B. H. 1997. Pile capacity by direct CPT and CPTu methods applied to 102 case histories. *Canadian Geotechnical J.* 34 (6): 886-904.

Fahey, M. 1998. Deformation and in-situ stress measurement. *Geotechnical Site Characterization*, Vol. 1 (Proc. ISC-1, Atlanta), Balkema, Rotterdam: 49-68.

Fellenius, B.H. 2001. The O-cell: an innovative engineering tool. *Geotechnical News Magazine*, Vol. 19 (2): 32-33.

Fleming, W G K, Weltman A J, Randolph M F and Elson W K. 1992. *Piling Engineering, 2nd Edition*, Blackie /Halsted Press - Wiley & Sons, London: 122-128.

Mayne, P W. 2005. Integrated ground behavior. in-situ and lab tests. *Deformation Characteristics of Geomaterials*, Vol. 2 (IS-Lyon), Taylor & Francis Group, London: 155-177.

Mayne, P.W. 2007a. In-Situ Test Calibrations for Evaluating Soil Parameters, *Characterization & Engineering Properties of Natural Soils*, Vol. 3, Taylor & Francis Group, London: 1602-1652.

Mayne, P W. 2007b. *Synthesis 368 on Cone Penetration Testing*, National Cooperative Highway Research Program (NCHRP), National Academy Press, Washington, DC: 117 p. www.trb.org

Mayne, P.W. and Woeller, D.J. 2008. O-cell response using elastic pile and seismic piezocone tests. *Proc. Intl. Conf. on Foundations* (Dundee), British Geotechnical Association, IHS BRE Press, UK.

O'Neill, M W, Brown, D A, Townsend, F C, and Abar, N. 1997. Innovative load testing of deep foundations. *Transportation Research Record No. 1569*, Washington, D.C.: 17-25..

O'Neill, M W and Reese L C. 1999. *Drilled Shafts: Construction Procedures and Design Methods*, Vols. I and II, Publication FHWA-IF-99-025, Assoc. Drilled Shaft Contractors, Dallas: 758 p.

Osterberg J O. 1998. The Osterberg load test method for bored and driven piles. *Proc. 7th Intl. Conf. Piling and Deep Foundations* (Vienna), Deep Foundations Institute, NJ: 1.28.1-1.28.11.

Osterberg, J O. 2000. Side shear and end bearing in drilled shafts. *New Technological and Design Developments in Deep Foundations*, GSP No. 100 (Proc. GeoDenver), ASCE, Reston, Virginia: 72-79.

Randolph M F and Wroth C P. 1978. Analysis of deformation of vertically loaded piles. *Journal of Geotechnical Engineering Division (ASCE)*, Vol. 104 (GT12): 1465-1488.

Randolph M F and Wroth C P. 1979. A simple approach to pile design and the evaluation of pile tests. *Behavior of Deep Foundations*, STP 670, ASTM, West Conshohocken, Pennsylvania: 484-499.

Senneset, K., Sandven, R. and Janbu, N. 1989. Evaluation of soil parameters from piezocone tests. *Transportation Research Record 1235*, National Academy Press, Washington, DC: 24-37.
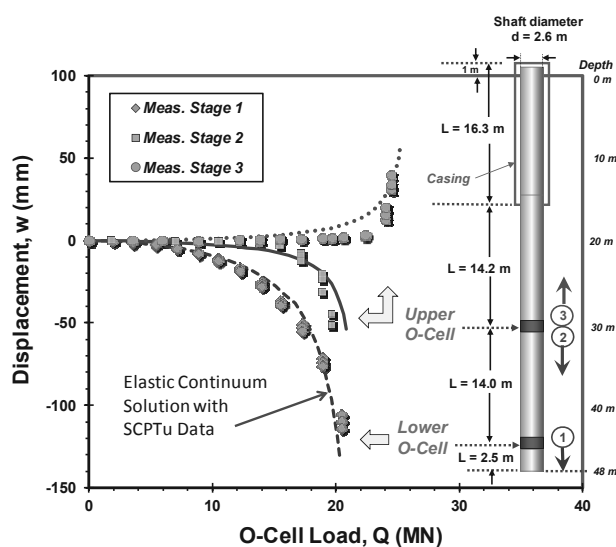
Figure 6. Measured and calculated O-cell response for test shaft MP-1 at Cooper River Bridge site

suggested for relatively insensitive clays, nonstructured soils, and uncemented quartzitic sands (Mayne 2007a). For the Cooper marl, the high calcium carbonate content would implicate a rather structured geomaterial, therefore an appropriate exponent "g" = 0.5 can be considered characteristic.

Using the aforementioned elastic continuum solution and axial pile capacity determined from CPT results, together with the initial shear moduli obtained from the V_s profile, the response of the three pile segments from the O-cell arrangements can be represented, as shown in Figure 6 for test shaft MP-1. A reasonable agreement is observed for all three loading stages of both O-cell jacks, including an approximate nonlinear load-displacement-capacity behavior.

If desired, a more realistic compressible pile solution is also available (Fleming et al. 1992), yet more complex as it involves a hyperbolic tangent function. In that case, the developed curves are quite similar to those shown herein.